

Variations in sediment provenance during the past 3000 years off the Tagus River, Portugal

Ulrich Alt-Epping^{a,*}, Jan-Berend W. Stuit^a, Dierk Hebbeln^a, Ralph Schneider^b

^a DFG-Research Center Ocean Margins, University of Bremen, PO Box 330440, 28334 Bremen, Germany

^b Department of Geosciences, Christian-Albrecht University Kiel, Ludewig-Meyn-Str. 10, 24118 Kiel, Germany

ARTICLE INFO

Article history:

Accepted 23 November 2008

Keywords:

organic matter provenance
nutrient budget
grain size
tsunami
NAO
Portuguese margin
Tagus River

ABSTRACT

Marine sediments from the Portuguese shelf are influenced by environmental changes in the surrounding continental and marine environment. These are largely controlled by the North Atlantic Oscillation, but additional impacts may arise from episodic tsunamis. In order to investigate these influences, a high resolution multi-proxy study has been carried out on a 5.4 m long gravity core and five box cores from the Tagus prodelta on the western Portuguese margin, incorporating geochemical (C_{org}/N_{total} ratios, $\delta^{13}C_{org}$, $\delta^{15}N$, $\delta^{18}O$, C_{org} and $CaCO_3$ content) and physical sediment properties (magnetic susceptibility, grain-size). Subsurface data of the five box cores indicate no major effect of early postdepositional alteration. Surface data show a higher fraction of terrigenous organic material close to the river mouth and in the southern prodelta. Gravity core GeoB 8903 covers the last 3.2 kyrs with a temporal resolution of at least 0.1 cm/yr. Very high sedimentation rates between 69 and 140 cm core depth indicate a possible disturbance of the record by the AD1755 tsunami, although no evidence for a disturbance is observed in the data. Sea surface temperature and salinity on the prodelta, the local budget of marine NO_3^- as well as the provenance of organic matter remained virtually constant during the past 3.2 kyrs.

A positive correlation between magnetic susceptibility (MS) and North Atlantic Oscillation (NAO) is evident for the past 250 years, coinciding with a negative correlation between mean grain-size and NAO. This is assigned to a constant riverine supply of fine material with high MS, which is diluted by the riverine input of a coarser, low-MS component during NAO negative, high-precipitation phases. End-member modelling of the lithic grain-size spectrum supports this, revealing a third, coarse lithic component. The high abundance of this coarse end-member prior to 2 kyr BP is interpreted as the result of stronger bottom currents, concentrating the coarse sediment fraction by winnowing. As continental climate was more arid prior to 2 kyr BP (Subboreal), the coarse end-member may also consist of dust from local sources. A decrease in grain-size and $CaCO_3$ content after 2 kyr BP is interpreted as a result of decreasing wind strength. The onset of a fining trend and a further decrease in $CaCO_3$ around AD900 occurs simultaneous to climatic variations, reconstructed from eastern North Atlantic records. A strong increase in MS between AD1400 and AD1500 indicates higher lithic terrigenous input, caused by deforestation in the hinterland.

© 2008 Elsevier B.V. All rights reserved.

1. Introduction

Climatic conditions over large parts of Europe are largely determined by the North Atlantic Oscillation (NAO), which describes the varying air-pressure gradient between the Azores High and the Iceland Low (e.g. Hurrell, 1995). Precipitation over the Iberian Peninsula correlates negatively with the NAO index (Trigo et al., 2004; Vicente-Serrano and Heredia-Laclaustra, 2004), whereas wind strength, which drives coastal upwelling along the Portuguese margin, shows a positive correlation with NAO (Oschlies, 2001). Although variations in NAO occur on short timescales, high local sedimentation

rates allow an assessment of the influence of the NAO on the marine sediment record.

Previous studies from the Tagus prodelta (Gil et al., 2006; Bartels-Jónsdóttir et al., 2006) could not reconstruct a synchronous timing of environmental periods (e.g. Little Ice Age or Medieval Warm Period). Depending on the literature source, the beginning and end of these periods vary considerably. Nevertheless, a prodelta record (Lebreiro et al., 2006) has been successfully correlated to records from the eastern and northern North Atlantic (Hebbeln et al., 2006; Eiriksson et al., 2006), showing synchronous environmental changes in south-west and northern Europe. Hence, despite the high spatial heterogeneity of sediment properties on the shelf, this suggests the existence of large scale driving mechanisms for environmental changes, e.g. by varying atmospheric circulation patterns.

* Corresponding author.

E-mail address: alt-epping@rcm-bremen.de (U. Alt-Epping).

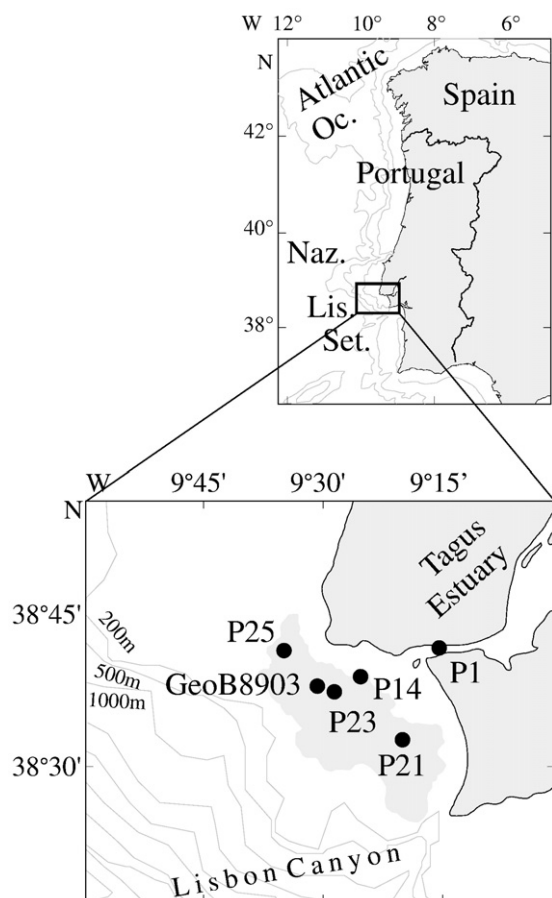


Fig. 1. Map of the area of investigation and sampling locations. Grey shaded area shows the mud belt redrawn after Jouanneau et al. (1998).

The sedimentary record off the Tagus Estuary on the central western Portuguese shelf combines of marine and continental inputs, as it is under the influence of seasonal coastal upwelling (Fiúza, 1983) and of continental contributions from the Tagus River and Estuary (Jouanneau et al., 1998). Additionally, aeolian or current-transported material may contribute to the sediments (e.g. Mahowald et al., 1999; Moreno et al., 2002). Past changes in the marine environment and in the continental hinterland as well as variations in atmospheric circulation intensity may therefore be recorded in these sediments. Because local sedimentation rates are high, the interaction between continental and marine environmental processes can be resolved on short timescales. Sediment parameters that are indicative of changes in continental and marine environment include elemental and stable carbon and nitrogen isotope ratios as proxies for organic matter provenance and NO_3^- budget (e.g. Thornton and McManus, 1994; Middelburg and Nieuwenhuize, 1998, for organic matter provenance; Altabet and Francois, 1994; Freudenthal et al., 2001, for $\delta^{15}\text{N}$ as proxy for nutrient utilisation) as well as planktonic foraminiferal $\delta^{18}\text{O}$ as proxy for sea surface temperature (SST) and salinity (SSS) (McCrea, 1950; Niebler et al., 1999; Wolff et al., 1999; Bonway and Mix, 2004). Inorganic sediment properties, such as grain-size and magnetic susceptibility (MS) are indicative for the depositional environment and sediment source. Particularly a detailed grain-size analysis, including modelling of potential end-members of the grain-size spectrum, allows the evaluation of different sources of the lithic sediment fraction (Stuut et al., 2002).

Additional to environmental changes, the AD1755 tsunami, which devastated the city of Lisbon, may have disturbed the coastal sediments significantly (Abrantes et al., 2005). Here, the high temporal

resolution of the shelf record helps in assessing a possible impact of the tsunami on the shelf sediments.

In this study a gravity core from the central part of the western Portuguese shelf is analysed with respect to its geochemical ($C_{\text{org}}/N_{\text{total}}$, $\delta^{13}\text{C}_{\text{org}}$, $\delta^{15}\text{N}$, $\delta^{18}\text{O}$, CaCO_3 content) and physical (grain-size, MS) sediment properties in order to evaluate environmental variations on the Iberian Peninsula and in the adjacent marine environment as well as sedimentological changes in the depositional area. The downcore information is complemented by surface and subsurface data from five nearby box cores, which yield information about the recent spatial distribution and possible early diagenetic alterations of the analysed parameters.

2. Regional setting

The central part of the western Portuguese margin is bordered to the North by the Nazaré Canyon and to the South by the Lisbon and Setúbal Canyons. These canyons intercept the ca. 20–30 km broad shelf and prevent large scale coast-parallel sediment transport.

The main source for continental sediments to the shelf is the Tagus River, which is 1000 km long and drains about 80600 km². It discharges into the Atlantic Ocean close to the city of Lisbon through a 350 km² large, mesotidal estuary. The Tagus Estuary is the third largest estuary in Europe and with sedimentation rates of around 80 cm/kyr (Freitas et al., 1999) it acts as a depocenter for river-transported sediments. The sediments discharged to the shelf are partly deposited on a ca. 550 km² large mud belt in front of the estuary mouth and partly transported further south to the Lisbon Canyon, through which they are discharged into the deep sea. The suspended matter, carried by the Tagus outflow can be traced by a bottom nepheloid layer, stretching over the Tagus mud belt and extending towards the Lisbon Canyon (Jouanneau et al., 1998).

Marine productivity is largely controlled by upwelling from May to September, which is driven by the periodic relocation of the Azores high-pressure system closer to the Iberian coast (Fiúza, 1983) and associated northerly winds. This causes upwelling of cold and nutrient rich waters from 60 to 120 m depth, generating a ca. 50 km wide high productivity zones along most parts of the Portuguese coast (Fiúza, 1983), occasionally extending offshore some hundreds of kilometers through filaments. Upwelling increases marine productivity to 60 to 90 gC/m²yr (Fiúza, 1983; Abrantes and Moita, 1999). During winter months the Azores High is located south off the northwest African coast, resulting in southerly winds, which favour downwelling conditions.

3. Materials and methods

A 5.4 m long gravity core (GeoB 8903) and five box cores (Plutur-1, 14, 21, 23, 25) with a length of between 7 and 20 cm were collected from the Tagus prodelta (Fig. 1, Table 1). Samples for elemental and

Table 1
List of analysed cores.

Core name	Latitude (Decimal °N)	Longitude (Decimal °W)	Water depth (m)	Length (m)	Project (sample holder)
Plutur1	38.692	9.261	19	0.2	
Plutur14	38.646	9.424	54	0.14	
Plutur21	38.545	9.337	101	0.15	OMEX I (IH)
Plutur23	38.622	9.477	100	0.09	
Plutur25	38.688	9.582	101	0.07	
GeoB 8903	38.631	9.514	102	5.4	SEDPORT (RCOM)

Compilation of investigated cores. IH: Hydrographic Institute, Lisbon, Portugal. OMEX: Ocean Margin Exchange. SEDPORT: Sedimentation processes on the Portuguese margin: the role of continental climate, ocean circulation, sea level and Neotectonics. RCOM: Research Center Ocean Margins, Bremen, Germany.

isotope analyses were taken every 5 cm from the gravity core, whereas the box cores were sampled in 1 cm steps.

The elemental C and N content was analysed following the procedure described by Müller et al. (1994) at the RCOM, Bremen. The freeze-dried sediment was ground and 25 mg of material was filled into tin containers and analysed in an Elementar Vario-EL3 element analyser to obtain the total carbon and nitrogen content. To measure organic carbon and nitrogen, 25 mg of sediment was filled into silver containers and treated with 1-molar HCL to remove carbonate. Samples were not washed after treatment to prevent the loss of suspended material (Schubert and Nielsen, 2000). The N content of carbonate-containing and carbonate-free samples was compared in order to detect offsets that might indicate loss of sediment material during treatment or effects of decarbonization on the N content. The offsets were all in a tolerable range (maximum rel. 3%), confirming only minor and non-systematic effects of decarbonization on the N content. Precision was ensured by continuous control measurements of a lab internal standard. The calcite content was calculated using the equation $\text{CaCO}_3 = 8.33 * (\text{C}_{\text{total}} - \text{C}_{\text{org}})$.

The isotopic composition of organic carbon ($\delta^{13}\text{C}_{\text{org}}$) was measured on carbonate-free samples. The material was combusted to CO_2 in a Heräus element analyser, cleaned in a trapping box system and measured with a Finnigan Delta E mass spectrometer against an internal standard gas, which was calibrated against NBS19. Absolute measuring error is $\pm 0.1\text{‰}$, based on long term calibration curves. Isotopic values are given in standard notation with reference to PDB. Nitrogen isotope ratios ($\delta^{15}\text{N}$) were measured by combusting bulk sediments in a Carlo Erba element analyser to N_2 , which was then led into the Finnigan Delta E mass spectrometer in a continuous flow mode, using He as carrier gas. Absolute precision is ± 0.2 to 0.3‰ , based on repetitive measurements. Internal calibration was performed the same way as for $\delta^{13}\text{C}$. Isotopic values are given in standard notation against $\delta^{15}\text{N}_{\text{air}}$ ($= 0\text{‰}$, Mariotti, 1983). The use of bulk sediment for nitrogen isotope analysis instead of decarbonized material is justified by the observation that decarbonization has no effect on the nitrogen isotopic composition (Lavik, 2001).

Grain-size was measured on gravity core GeoB 8903 every 5 cm with a Coulter LS200 on bulk and terrigenous material, resolving grain-size spectra between 0.4 and 2000 μm . Bulk sediment of the top 55 cm was additionally measured on a 1 cm resolution. The terrigenous fraction was obtained by treating bulk sediment with 10 ml 10% hydrochloric acid to remove CaCO_3 , 10 ml 35% hydrogen peroxide to remove organic matter and 6 mg sodium hydroxide (NaOH) to remove biogenic opal. All samples were dispersed with sodium pyrophosphate ($\text{Na}_4\text{P}_2\text{O}_7 \cdot 10\text{H}_2\text{O}$) prior to measurement. Mean grain-sizes were calculated with the software GRADISTAT (Blott and Pye, 2001) after the Folk and Ward (1957) method. End-member modelling allowed the distinction between several possible lithic subpopulations of the grain-size spectrum (Weltje, 1997). This is based on the concept, that the terrigenous fraction of deep-sea sediments in the ocean, which are not disturbed by post-depositional processes, can be considered a mixture of ice-rafted, wind-blown, and fluvial sediments. This mixture can be unmixed into subpopulations, so-called end members that can be assigned to sediment-transport mechanisms (Prins, 1999; Stuet et al., 2002; Weltje and Prins, 2003; Holz et al., 2004). In this study we have also followed this end-member approach, to try and explain the variability in the grain-size distributions of the terrigenous sediment fraction on the Portuguese continental slope.

The minimum number of end members required for a satisfactory approximation of the data is calculated from the goodness-of-fit statistics, represented by the coefficients of determination. The coefficient of determination represents the proportion of the variance of each grain-size class that can be reproduced by the approximated data. This proportion is equal to the squared correlation coefficient (R^2) of the input variables and their approximated values (Weltje, 1997; Prins and Weltje, 1999). Hence, the eventual outcome of the

model is a statistically unique solution with end members that represent real particle-size distributions. The only prescription that is used during modelling is the fact that end members may not have negative grain sizes. No predefinitions are made regarding shape, sorting or modal sizes of the end members (for more details of the application of the model to particle-size distributions see: Weltje and Prins, 2003).

Magnetic susceptibility (MS) was measured on gravity core GeoB 8903 in 1 cm steps with a GEOTEK Kappabridge at the RCOM, Bremen.

The age model of core GeoB 8903 is based on ten ^{14}C AMS datings. Dated samples contained between 3.9 and 7.5 mg of multispecies planktonic foraminifera and were measured at the Leibniz Laboratory of the University Kiel, Germany (Nadeau et al., 1997) (Table 2). Radiocarbon ages were corrected for a reservoir effect of 400 years (Abrantes et al., 2005), regardless of biasing influences of changing upwelling or river freshwater discharge. The results were calibrated with the software Calib 5.0.1 (Stuiver and Reimer, 1993), using the "intcal04" calibration curve.

4. Results

4.1. Plutur box cores

The box cores contain between 1.3 and 1.7 wt.% C_{org} , with higher values (2.1 wt.%) in the upper 4 cm of core Plutur-1 (Fig. 2). The N_{total} content decreases downcore in a parallel way in all five cores from between 0.15 and 0.19 wt.% at the core tops to ca. 0.13 wt.%. The CaCO_3 content is constant within each core, varying between 4 wt.% in the box core most proximal to the estuary (Plutur-1) and 16 wt.% in the distal box core (Plutur-25). However, Plutur-23, which is located on the shelf south of the estuary mouth, shows intermediate CaCO_3 values between Plutur-14 and Plutur-23. $\text{C}_{\text{org}}/\text{N}_{\text{total}}$ ratios increase slightly with depth, ranging between 8 and 10 at the core tops and between 9 and 10 at the core bases. Plutur-1 shows a high variability, with $\text{C}_{\text{org}}/\text{N}_{\text{total}}$ values of up to 12 in the upper 4 cm and at 20 cm depth. The $\delta^{15}\text{N}$ values show a comparable, decreasing pattern with increasing distance to the estuary mouth. Plutur-1 shows highest $\delta^{15}\text{N}$ values of around 7‰, Plutur-21, Plutur-23 and Plutur-25 show similar values between 5 and 6‰ (Fig. 2). The $\delta^{13}\text{C}_{\text{org}}$ of the box cores decreases clearly towards the estuary mouth, ranging from -22.5‰ in Plutur-25 to -26‰ in Plutur-1.

4.2. GeoB 8903

C_{org} content (Fig. 3E) is ca. 1 wt.% below 500 cm, before increasing to 1.4 wt.% between 470 and 300 cm and further to 1.6 wt.% between 300 and 250 cm. A decrease to 1.4 wt.% at 170 cm is followed by constant values until 50 cm, above which C_{org} content increases to 1.6 wt.% at the core top. $\text{C}_{\text{org}}/\text{N}_{\text{total}}$ ratios (Fig. 3D) are around 10.5

Table 2
Dated samples of core GeoB 8903.

Depth (cm)	^{14}C age (yrs BP)	Calibrated (yrs BP)	Age (yrs AD)	Half error (yrs)	Sed. rate (cm/yr) (interval, cm)
10	Modern	Modern	Modern		0.2 (0–10)
51	610	170	1780	18.5	0.25 (10–51)
69	735	350	1600	18	0.1 (51–69)
140	760	360	1590	40	10.21 (69–140)
172	685	405	1545	24.5	0.7 (140–172)
198	760	455	1495	30	0.48 (172–198)
248	1035	580	1370	17.5	0.41 (198–248)
333	1660	1220	730	44.5	0.13 (248–333)
413	2000	1480	470	88.5	0.31 (333–413)
498	2885	2580	– 630	144	0.08 (413–498)

Compilation of dated samples and dating results. ^{14}C ages are corrected by 400 yrs reservoir effect (Abrantes et al., 2005) and calibrated with Calib5.0.1, using the "intcal04" calibration dataset (Stuiver and Reimer, 1993).

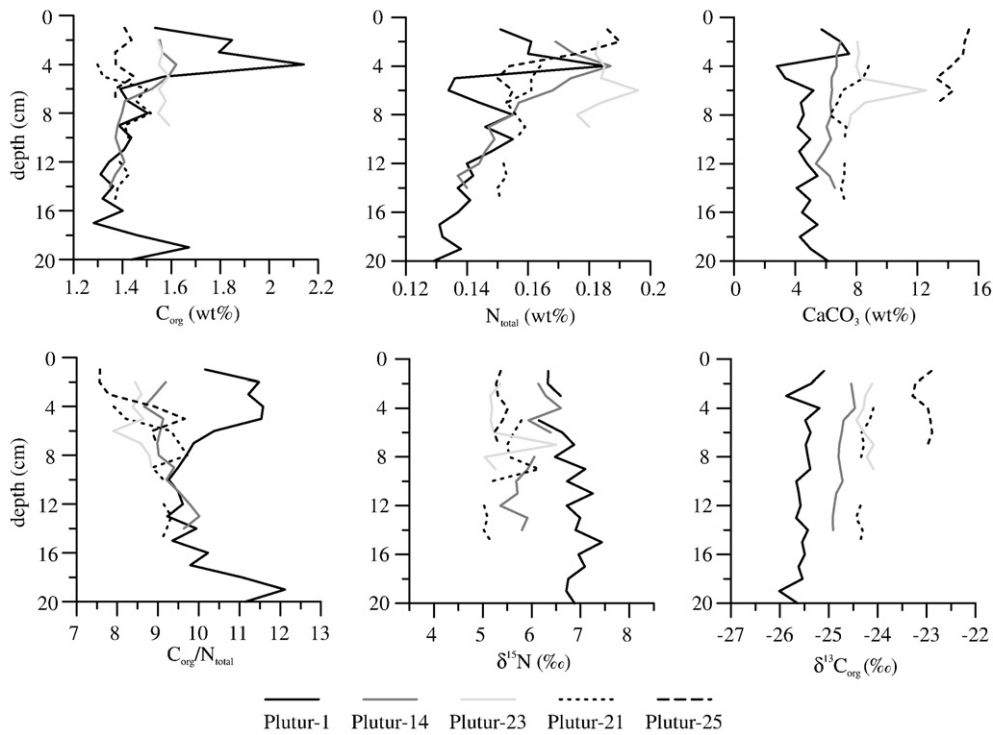


Fig. 2. Data of the five Plutur box cores.

between 450 cm and the core base before they increase to a maximum value of 11 at 450 cm. Above 450 cm the C_{org}/N_{total} values decrease to around 9.5 at the core top. This trend is interrupted by two intervals of relatively constant C_{org}/N_{total} values between 350 and 250 cm and between 170 and 100 cm. $\delta^{13}C_{org}$ values (Fig. 3C) vary between -23.2

and -24% , with heavier values around 470 cm, between 370 and 300 cm and above 60 cm. Relatively light $\delta^{13}C_{org}$ values are observed below 490 cm, between 450 and 400 cm and between 230 and 60 cm. $\delta^{15}N$ values (Fig. 3B) vary between 5 and 5.8‰ with slightly heavier values and three positive peaks between 350 and 250 cm. At 150 cm a

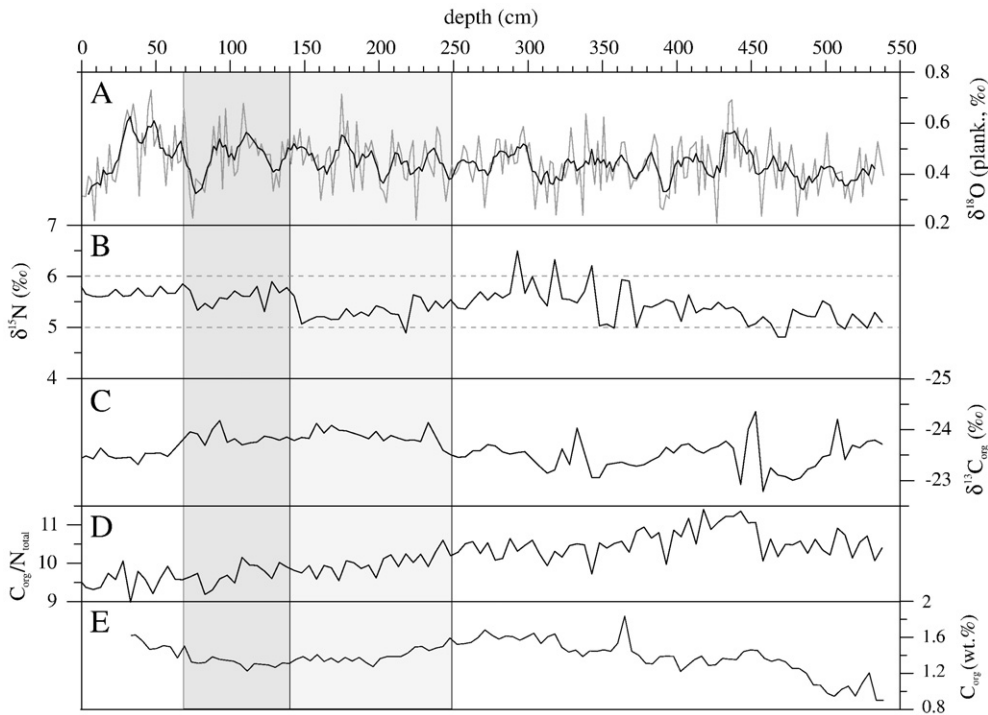


Fig. 3. Selected sediment parameters (from top to bottom: planktonic $\delta^{18}O$, $\delta^{15}N$, $\delta^{13}C_{org}$, C_{org}/N_{total} ratios, C_{org} content), which are indicative for oceanographic conditions (SST and SSS variations, nutrient budget) and organic matter provenance. Red line in the $\delta^{18}O$ plot shows the 9-point running average. Dashed, horizontal lines in $\delta^{15}N$ plot indicate upper and lower limits of typical deep water $\delta^{15}NO_3^-$ (5–6‰, Liu and Kaplan, 1989).

sharp increase from 5.2 to 5.6‰ is observed, otherwise variations in $\delta^{15}\text{N}$ are minor. The CaCO_3 content (Fig. 4D) decreases from 24 wt.% at the core base to 14–18 wt.% between 470 cm and 300 cm. Above 300 cm the CaCO_3 content decreases to 10 wt.% at 170 cm and remains constant until the core top.

The MS of core GeoB 8903 (Fig. 4B) is below 5×10^{-5} until 320 cm interrupted by two positive peaks between 470 and 480 cm and around 400 cm to values around 10×10^{-5} and 5×10^{-5} , respectively. At 320 cm MS increases to ca. 10×10^{-5} , before increasing further to $30\text{--}35 \times 10^{-5}$ from 250 to 200 cm. This high level is maintained until the core top, interrupted by a short excursion to 25×10^{-5} at 140 cm.

The $\delta^{18}\text{O}$ values (Fig. 3A) range between 0.2 and 0.7‰ and thus vary not significantly, except for a constant decline from 0.6‰ to 0.3‰ in the top 30 cm.

Mean bulk grain-size of core GeoB 8903 (Fig. 4A) decreases from 24 μm at the core base to 15 μm around 450 cm core depth, fluctuating around this value until 240 cm. Two slight increases in mean grain-size are observed around 420 cm (20 μm) and 320 cm (18 μm). Above 240 cm, values decrease to 10 μm until the core top. The mean grain-size of the terrigenous sediment fraction is similar, with ca. 1–2 μm finer values between 420 cm and the core base (Fig. 4A).

End-member modelling of the grain-size spectrum of the terrigenous sediment fraction results in several potential lithic subpopulations. With two subpopulations, 77% of the variance of the grain-size spectrum can be explained. Three end-members give a correlation coefficient R^2 of 0.86, whereas four end-members results in an only slightly improved correlation coefficient of 0.91. Therefore, the three end-member model is chosen to explain the sediments grain-size distribution in an optimal way. End-member 1 (EM1) is defined as the finest subpopulation, which is poorly sorted with a mean grain-size of 6 μm (Fig. 5A). End-member 2 (EM2) has a mean grain-size of 12 μm , end-member 3 (EM3) has a mean grain-size of 25 μm and is better sorted. These values apply for the low resolution model (5 cm spacing), but are equal for the separately obtained high resolution model (1 cm spacing), showing the good reproducibility of the modelling results. The abundance of each end-member changes with depth, showing a max. 80% abundance of EM3 in the lowest 80 cm and an increased EM3 fraction of ca. 60% between 350 and 300 cm (Fig. 5B). Above 300 cm, the fraction of EM3 decreases to below 20% at 200 cm and to around 10% at the core top. EM2 shows generally an abundance of around 40%, with lower values below 470 cm, higher values between 470 and 340 cm and again lower

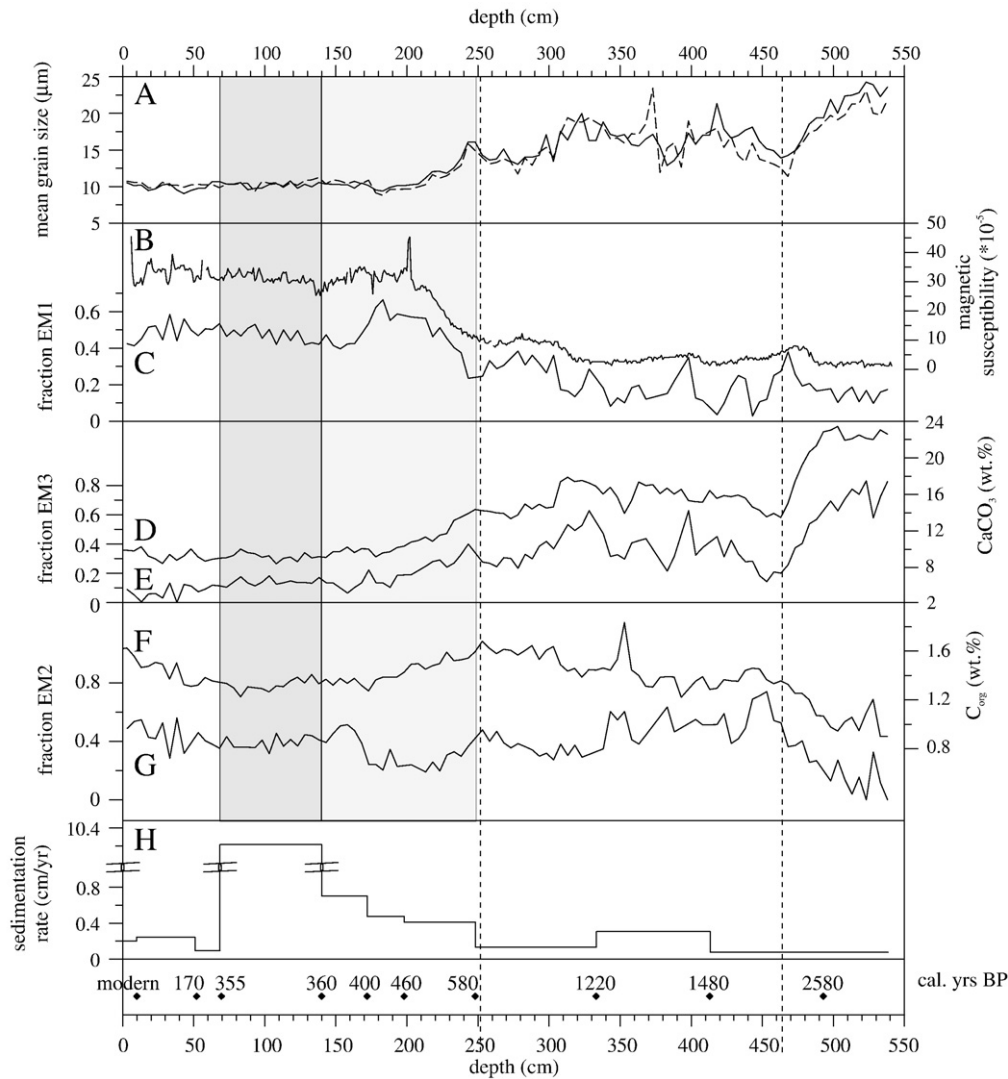


Fig. 4. Compilation of sediment data versus age. (A) Mean grain-size (bulk sediment: solid line, terrigenous fraction: dashed line), comparison between MS and EM1 (B, C), between CaCO_3 content and EM3 (D, E) and between C_{org} and EM2 (F, G). Sedimentation rates (H) and datings are shown below. The interval, which is omitted from interpretation, is shaded in dark grey, whereas the light grey box marks the section, in which a tsunamigenic influence cannot be excluded. Dashed lines separate the three identified phases, which are described in the text.

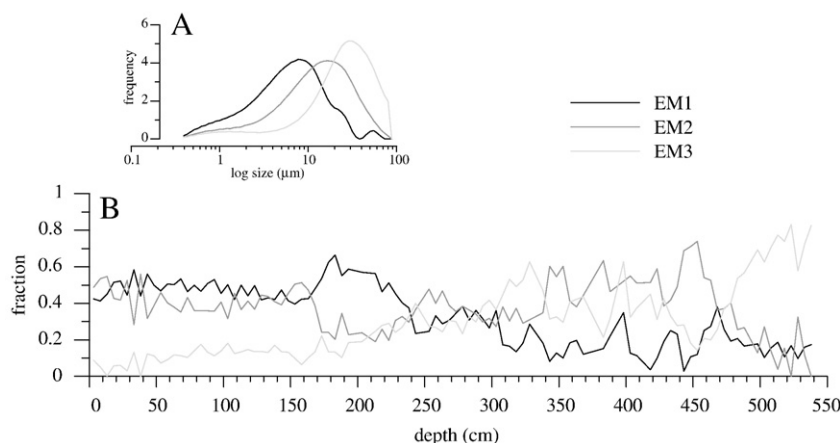


Fig. 5. Grain size spectra of the three modelled end-members (A) and downcore variation of the end-members (B).

values between 220 and 170 cm. EM1 comprises a low abundance in the lower half of the record (10–30%) and values between 40 and 70% above 240 cm (Fig. 5B).

The reservoir corrected and calibrated age model of core GeoB 8903 (Table 2, Fig. 6A, B) has an oldest date of 628BC close to the base of the core. Resulting sedimentation rates (SR) are with 0.08 cm/yr lowest in the bottom part of the core before they increase to 0.3 cm/yr between 413 and 333 cm depth. Until 248 cm SR reach 0.13 cm/yr and increase to 0.1–0.7 cm/yr in the upper 248 cm. These sedimentation rates are in accordance to values reported by Jouanneau et al. (1998) and Abrantes et al. (2005) from the Tagus prodelta. A sedimentation rate of 10 cm/yr between 69 and 140 cm is probably unrealistic and discussed below.

5. Discussion

5.1. Plutur box cores

Decreasing C_{org}/N_{total} values as well as increasing $\delta^{13}C_{org}$ and $CaCO_3$ values along the transect Plutur-1–Plutur-14–Plutur-23 imply a decreasing terrigenous organic matter content with increasing distance from the estuary mouth. Furthermore, decreasing $\delta^{15}N$ values

indicate lower amounts of estuarine organic matter further offshore (Owens, 1985). Plutur-25, located in the northwestern part of the prodelta, shows typical marine properties (high $CaCO_3$ content, heavy $\delta^{13}C_{org}$). Plutur-21, located in the southern part of the prodelta, shows intermediate values similar to Plutur-23, implying that the sampling location is within a transport pathway for terrigenous sediment from the estuary to the Lisbon Canyon (Jouanneau et al., 1998).

The slight downcore increase of C_{org}/N_{total} ratios reflects the degradation of labile, N-rich organic substances, such as proteins, which is caused by a decrease in N_{total} (not shown). Isotope ratios are constant, showing no downcore trend and thus no sign for early diagenetic alterations.

The high variability of the data of Plutur-1 is caused by its location inside the estuary channel, where current speeds are highest and the sediment surface is frequently disturbed by anthropogenic activities (e.g. dredging) or natural processes (e.g. channel migration).

5.2. GeoB 8903

5.2.1. Age model

The complete recovery of the core top of gravity core GeoB 8903 is indicated by a post-AD1950 radiocarbon age at 10 cm core depth

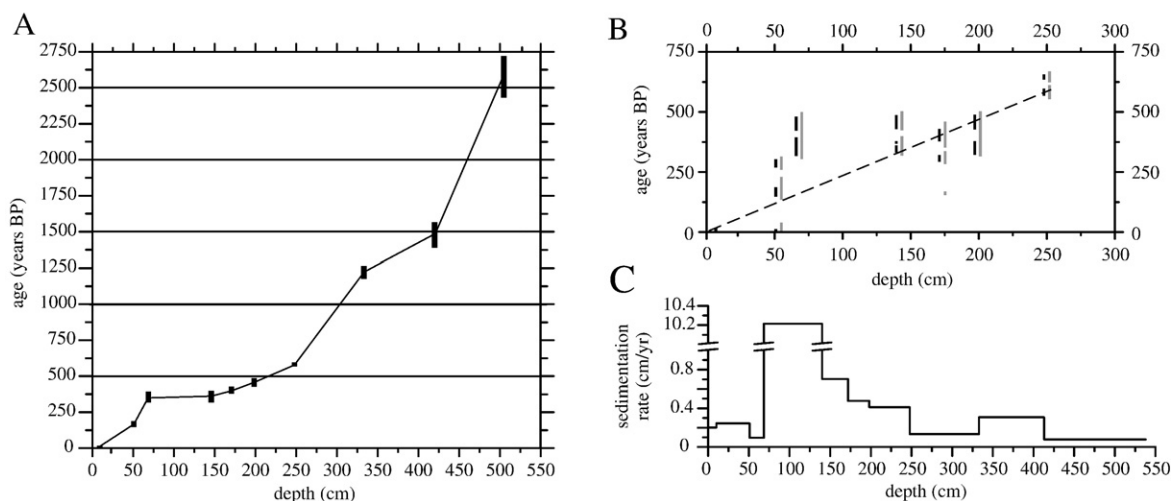


Fig. 6. Age model (A and B) and sedimentation rates (C) for core GeoB 8903. (A) shows calibrated (Stuiver and Reimer, 1993) and reservoir corrected (400 years, Abrantes et al., 2005) ages. Length of bars represents the dating error. (B) shows the enlarged dating results of the upper part of the sediment record. Black bars indicate the 1 sigma interval, grey bars the 2 sigma intervals. The length of each bar represents the probability for each date. (C) shows sedimentation rates.

as well as by a similar magnitude and pattern in MS in a nearby, ^{210}Pb -dated box core (Abrantes et al., 2005).

Four datings between 69 and 198 cm result in an identical range of possible ages between 300 and 490 cal. yrs BP (Fig. 6A, B). Particularly the 69 cm-dating results in an age reversal, suggesting a disturbance of the sedimentary record in this interval, which is possibly caused by the AD1755 tsunami. In that case, the 51 cm-dating level represents the upper limit of the tsunamigenic sediment layer. The definition of the lower boundary is problematic, because although the four datings are all in a similar range, suggesting a lower boundary of the tsunamigenic layer of at least 198 cm core depth, it is possible to construct a plausible linear age-depth relation between 140 and 248 cm (Fig. 6B). Omitting the 51 cm- and the 69 cm-datings, this line also intersects the origin and the resulting sedimentation rates of less than 0.7 cm/yr are in a very realistic range for this region (Jouanneau et al., 1998; Abrantes et al., 2005). Furthermore, the strong change in MS between 250 and 200 cm (Fig. 4B) is visible in other cores along the central Portuguese margin (e.g. Abrantes et al., 2005, Abrantes, pers. comm.) and therefore not an artefact of the tsunami. Hence, the interval 51–140 cm might well be disturbed and the interval 140–248 cm should be interpreted carefully, especially above 198 cm.

Grain-size and MS data in a gravity core from the southern prodelta indicates erosion of 39 cm sediment and subsequent, instantaneous deposition of 19 cm sediment, which has been explained by the AD1755 tsunami (Abrantes et al., 2005). However, sediment parameters of core GeoB 8903 show no evidence for a similar disturbance (Figs. 3 and 4). Particularly the grain-size is constant in this interval, which is similar to observations by Andrade et al. (2003) from inside the Tagus Estuary, stating that the tsunami left no relevant textural contrast in the sediments. Furthermore, Baptista et al. (2003) modelled a tsunami wave height of around 5 m at Oeiras, close to Lisbon outside the Tagus Estuary. This is relatively low, considering the shallow water depth and compared to a 12 m high tsunami wave at C. San Vicente, SW Portugal (Baptista et al., 2003). Due to the possible overestimation of the tsunamigenic impact on the shelf sediments and because in core GeoB 8903 neither grain-size nor MS data indicate a tsunami impact, the age model is applied according to Fig. 6A and Table 2. The interval 51–140 cm is omitted from interpretation, accounting for the extreme sedimentation rates and the interval 140–248 cm is regarded with care, as a tsunamigenic disturbance cannot be excluded.

5.2.2. Hydrography, organic matter provenance and nutrient conditions

Planktonic foraminifera $\delta^{18}\text{O}$ values show no significant variability, indicating no major variations in SST and SSS during the past 3.2 kyrs (Fig. 3A). Also sedimentary $\delta^{15}\text{N}$ values show no major variations, indicating a constant relation between nutrient supply (i.e. upwelling intensity) and nutrient consumption (i.e. marine productivity) as well as no varying influences of $\delta^{15}\text{N}$ affecting processes, such as e.g. denitrification or N_2 -fixation (Fig. 3B).

$\delta^{13}\text{C}_{\text{org}}$ and $\text{C}_{\text{org}}/\text{N}_{\text{total}}$ values in core GeoB 8903 are similar to those of the marine dominated core Platur-25, indicating a dominantly marine origin of organic matter. During the past 3.2 kyrs, $\text{C}_{\text{org}}/\text{N}_{\text{total}}$ ratios and $\delta^{13}\text{C}_{\text{org}}$ values vary only insignificantly in terms of organic matter provenance, implying a constant mixture of terrigenous and marine organic matter sources (Fig. 3C, D). No effects of the major historical climatic periods, such as Roman Warm Period, Dark Ages, Medieval Warm Period or Little Ice Age, nor of anthropogenic impacts on the continental environment (e.g. by deforestation) are recorded by the organic matter provenance proxies. A reason for this may be the reworking and partial deposition of terrigenous organic material within the Tagus Estuary, leading to reported, high sedimentation rates inside the estuary (Jouanneau et al., 1998). A turbidity maximum in the uppermost estuary (Castanheiro, 1982) indicates flocculation of dissolved riverine organic matter, triggered by the salinity increase, which can lead to the deposition of considerable parts of the riverine

organic material inside the estuary. Furthermore, variations in freshwater discharge should be recorded in planktonic $\delta^{18}\text{O}$ data, but the observation of constant SSS on the prodelta indicates thorough mixing of fresh- and seawater inside the estuary. This dilutes the terrigenous signal and leads to the relatively strong marine signature in the sediments close to the estuary mouth.

5.2.3. Grain size analyses

The similarity of the mean grain-size records of the bulk and terrigenous sediment fractions (i.e. carbonate, biogenic opal and organic matter removed) of core GeoB 8903 implies a dominance of lithic material. The positive correlation between CaCO_3 concentration, MS and mean grain-size further suggests, that the calcareous material is relatively coarse, whereas the finer sediment has a higher MS (Fig. 4A).

This is supported by the downcore abundance of the finest end-member EM1 (6 μm average grain size), which shows an excellent correlation with MS ($R^2 = 0.9$), implying a continental origin (Fig. 4B, C). Further, the fine and poorly sorted grain size spectrum of EM1 indicates a fluvial transport (Koopmann, 1981; Stuut et al., 2002; Holz et al., 2004). EM2 shows some similarity with C_{org} content (Fig. 4F, G), if the interval from 180 to 350 cm is omitted ($R^2 = 0.54$), but as there are no clear correlations between EM2 and provenance proxies visible, no definite statements about the origin of EM2 can be made. The coarsest end-member EM3 (25 μm) is strongly related to CaCO_3 content ($R^2 = 0.92$) (Fig. 4D, E). These findings confirm, that the calcareous fraction is related to coarse sediment material (EM3) and that the MS signal is related to the fine fraction (EM1). The lithic character of EM3 indicates a non-marine origin, but fluvial transport would generate a poorly sorted grain-size spectrum, which is not observed here. However, winnowing due to e.g. stronger bottom currents can concentrate and sort the EM3 fraction, particularly prior to 2 kyr BP (below 450 cm core depth) (Figs. 3E and 5). Winnowing is supported by low sedimentation rates in the lower part of the sedimentary record, as well as by the reconstruction of stronger bottom-currents on the northwestern Portuguese shelf prior to 2.2 kyr BP (Martins et al., 2006). As current intensity is related to wind strength, an aeolian origin for EM3 is plausible as well. Dry climate at that time supports the input of dust, possibly originating from the central Iberian Peninsula, as suggested by the relatively coarse average grain-size. Dust may also be derived from the Saharan desert, from where dust is transported northwards over the Iberian Peninsula (Guerzoni et al., 1997; Moreno et al., 2002), which is well observed by SeaWiFS satellite images.

The coevally high CaCO_3 content is thereby caused by winnowing, rather than by changes in marine production, because the latter should also be observed in the C_{org} content.

Physical sediment properties show a high spatial variability on the Tagus prodelta. This is for example evidenced by large differences in grain-size between core GeoB 8903 and a sediment record from the south-eastern prodelta, 17 km away (Lebreiro et al., 2006). In the latter core, grain-sizes range between 30 and 100 μm and sand content is between 20 and 75%. Combined with the differences regarding the record of the AD1755 tsunami, which were discussed earlier, this emphasises the textural variability of sediments on the Tagus mud belt and on the shelf.

5.2.4. Relation to NAO

On a short timescale, i.e. for the past 250 years, the proxy data of GeoB 8903 can be compared to NAO reconstructions, to evaluate a potential influence of NAO variations on sediment properties. Prior to AD1750 limitations of the age model and possible disturbances of the sedimentary record prevent a reliable correlation of the sediment record with NAO reconstructions. Furthermore slight offsets in sampling depth between MS measurements and grain-size analyses may lead to a shift between both records between 35 and 55 cm.

MS shows a positive correlation with a reconstructed NAO index (Cook et al., 2002), i.e. low MS during NAO negative phases (Fig. 7). Simultaneously a negative correlation between mean bulk grain size and NAO is evident. MS is interpreted as proxy for terrigenous sediment supply and should thus increase during negative NAO (i.e. high river runoff). However, the apparent contradiction can be explained by the existence of two distinct, lithic subpopulations, of which the finer carries the MS signal. The input of coarser, non-susceptible particles to the shelf by stronger currents and higher suspended sediment load during NAO negative phases dilutes the high-MS signal and leads to the observed positive correlation between NAO and MS as well as to the negative correlation between NAO and mean bulk grain-size (Fig. 7). The furthermore excellent correlation between EM1 and MS allows the classification of EM1 as fine subpopulation, which appears to be supplied to the shelf constantly. The coarser, magnetically non-susceptible subpopulation is accordingly represented by EM2 (Fig. 5A).

This concept is further supported by weak, but evident correlations between NAO index and endmember abundance (Fig. 8). EM1 shows both a positive correlation with NAO, whereas EM2 correlates negatively with NAO. The correlation between EM3 and NAO is very weak, but best visible below 20 cm depth. Due to the low relative abundance, this end-member is most susceptible to small variations in sediment input. Hence, only slight fluctuations in the supply of EM3 can prevent an obvious correlation. Furthermore, as the abundances are given in a relative way, dilution effects also play a role and might weaken possible correlations with NAO. Thus, although these correlations are relatively weak, they show the dependence of individual sediment components on NAO.

A general conclusion from these observations is, that the sediment texture is an essential factor, which must be considered in paleoenvironmental interpretations. Typical proxies, which are used for paleoenvironmental reconstructions (MS, C_{org} content, $CaCO_3$ content), heavily depend on grain-size and are associated to distinctive components of the total sediment.

5.2.5. Long term variations

The part of the sediment record, which is not affected by the tsunami, shows three distinct phases. The oldest phase prior to 2 kyr BP is characterised by enhanced $CaCO_3$ content, coarser grain-sizes

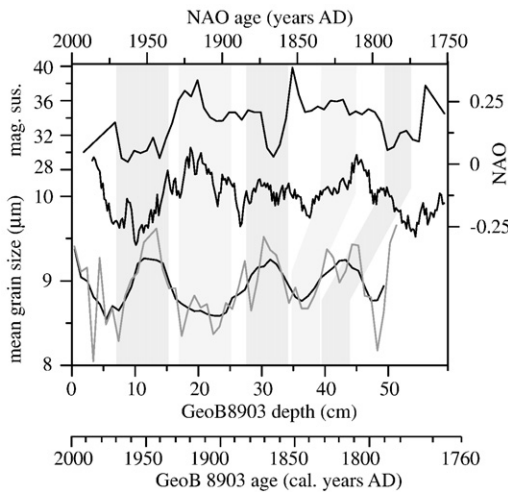


Fig. 7. Comparison of a NAO reconstruction (Cook et al., 2002: 33-point running average) with MS and mean grain-size (grey line: data in 1 cm resolution; black line: 5-point running average), showing the positive correlation between NAO and MS and the negative correlation between NAO and grain-size, as indicated by the plus and minus labels. The bottom time line indicates the age of the GeoB 8903 record at the respective depth. Prior to AD1750 the age model is uncertain, preventing a reliable correlation between the sediment record and NAO.

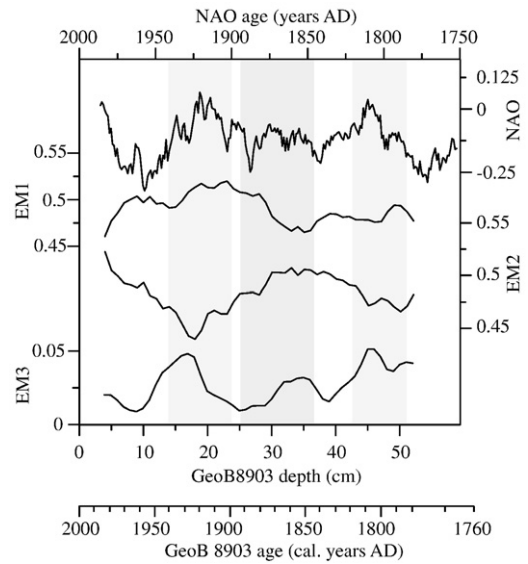


Fig. 8. Comparison of a NAO reconstruction (Cook et al., 2002: 33-point running average) with end-member abundances (7-point running average), showing a weak but significant positive correlation between EM1 and EM3 and NAO, whereas EM2 and NAO correlate negatively.

and a dominance of EM3 against EM1 and EM2 on one hand and lower C_{org} content on the other hand (Figs. 4 and 5). Interpreting EM3 as related to wind strength, regardless whether it is of aeolian origin or concentrated by winnowing due to strong shelf bottom currents, this observation implies a stronger wind energy during this phase. An aeolian origin is supported by the high availability of dust due to the prevailing dry climate. Increased shelf bottom-currents are additionally supported by a study from the northwestern Portuguese shelf (Martins et al., 2006).

The second period between 2 and 0.5 kyr BP is characterised by lower $CaCO_3$ content, finer grain-sizes, less EM3 with respect to EM2 and slightly higher C_{org} concentrations (Figs. 4 and 5). Corresponding to the above concept, this is explained by decreased wind energy, which results in weaker bottom-currents, hence less winnowing and a higher C_{org} concentration. Between 1.1 kyr BP and 0.6 kyr BP grain-sizes and $CaCO_3$ content decrease further, whereas MS increases slightly. Sedimentary records from the Eastern North Atlantic, e.g. from the Skagerrak (Hebbeln et al., 2006) and from other locations in the north-eastern North Atlantic (e.g. Eiriksson et al., 2006) show a coincident change around 1.1 kyr BP, evidenced by a coarsening and an increase in Ca/K ratio (Hebbeln et al., 2006). This is explained by a strengthening of bottom-currents (Hebbeln et al., 2006), induced by a reorganisation of atmospheric circulation patterns around 1.1 kyr BP (Scourse et al., 2006). This reorganisation may affect sedimentary records from southwestern Europe in a complementary way.

The youngest phase is characterised by a strong increase in lithic, terrigenous supply between 0.6 kyr BP and 0.5 kyr BP, evidenced by an abrupt increase in MS, remaining on a high level until the core top (Fig. 6B). If this was a climatically induced change, e.g. by a temperature decline due to the onset of the Little Ice Age (e.g. Lebreiro et al., 2006), MS should return to “warm” values in the top part, when temperatures are rising again. As this is not the case, the MS increase is interpreted as a permanent environmental change in the river catchment, e.g. caused by deforestation, which reached a maximum in the 15th and 16th century. During these times large amounts of timber were required, e.g. for shipbuilding. This interpretation is supported by a decreased influx of pollen from temperate trees (deciduous forests) since ca. 0.55BP (AD1400) in northwest Iberia (Desprat et al., 2003) indicating a regional decline in forest area. As a result, erosion rates and thus the discharge of lithic material through the Tagus River increased.

Consequently, the correlation of the GeoB 8903 record to historical climatic phases like Little Ice Age, Medieval Warm Period, Dark Ages or Roman Warm Period appears to be not appropriate. Instead, the observed changes in sediment parameters imply a different chronology of environmental changes, with the transition from a warm and dry period (possibly equivalent to the Subboreal) to a cool and wet period (possibly equivalent to the Subatlantic) dominating.

6. Summary

The sedimentary record of gravity core GeoB 8903 from the prodelta of the Tagus River on the central western Portuguese shelf shows environmental changes on a high temporal resolution, although the AD1755 tsunami possibly disturbed an at least 70 cm long section of the core. Variations in environmental conditions are evident by changes in physical sediment properties, rather than organic matter provenance or SST or SSS variations. Detailed grain-size analyses exhibit three end-members of the lithic sediment fraction. The finest end-member EM1 carries the MS signal and is interpreted due to its fine grain-size of average 6 μm to be of fluvial origin. A medium-sized end-member (EM2, mean grain-size 12 μm) is associated to the C_{org} content, whereas the third end-member (EM3, 25 μm) correlates strongly with CaCO_3 concentrations. The positive correlation between NAO and MS during the past 250 years and the coinciding negative correlation between mean bulk grain-size are explained by a perennial supply of EM1, diluted by an input of EM2 during NAO-negative phases. Hence, both sediment components are ascribed to fluvial, continental origin. The lithic composition and the relatively coarse, well-sorted grain-size spectrum of EM3 suggest an aeolian or fluvial origin. Generally the effect of NAO on the sediments appears to be weak and restricted to small variations in sediment composition. These are evident by slightly stronger EM2 inputs, related to increased precipitation rates during NAO negative phases or by a higher EM3 fraction during NAO positive phases, which are characterised by higher wind intensity. It becomes further evident, that proxies, that are commonly applied for paleoenvironmental reconstructions strongly depend on grain-size and that they are associated to specific sedimentary subpopulations.

The higher relative abundances of EM3, higher CaCO_3 content, coarser grain-sizes and the lower C_{org} content prior to 2 kyr BP are interpreted to be results of stronger winds, combined with continental aridity (Subboreal equivalent), increasing the availability of dust. As C_{org} is connected to finer material, it is winnowed by increased bottom-currents.

Complementary, a more humid, less windy climate between 2 and 0.5 ky BP is reflected by finer grain-sizes, less EM3, less CaCO_3 and a higher C_{org} content.

Around 0.6 to 0.5 kyr BP increasing deforestation in the catchment of the Tagus River, possibly triggered by the increasing demand for timber for shipbuilding, results in an increased supply of lithic material to the prodelta, indicated by strongly and permanently increased MS and by higher sedimentation rates.

The sedimentary record is possibly disturbed, as indicated by very high sedimentation rates between 69 and 140 cm and by a questionable age model between 51 cm and 198 cm. This covers the AD1755 tsunami. However, no textural or geochemical difference is visible between disturbed and undisturbed sediments, which is in accordance to observations from inside the Tagus Estuary (Andrade et al., 2003), but contrary to observation from the south-eastern prodelta (Abrantes et al., 2005). This and a completely different sediment texture compared to the south-eastern prodelta record emphasises the heterogeneity of sedimentation conditions and sediment properties on the Tagus prodelta and Tagus mud belt. Nevertheless, the timing of the observed change in sediment properties corresponds to the transition from a warm and dry period, which may be equivalent to the Subboreal, to a cooler and wetter phase, which

may be equivalent to the Subatlantic. Additionally, variations in sediment properties appear to be synchronous to environmental changes, that have been reconstructed from eastern North Atlantic records (e.g. Hebbeln et al., 2006), evidenced by complementary patterns in sediment parameters, such as grain-size, in records from these locations. This emphasises the significance of the GeoB 8903 record despite the high spatial variability of sediment properties and although the chronology of Little Ice Age, Medieval Warm Period, Dark Ages or Roman Warm Period, which is commonly applied to the Portuguese shelf records, can not be implemented here.

Acknowledgements

The work was conducted as a part of the SEDPORT project (Sedimentation Processes on the Portuguese margin: The Role of Continental Climate, Ocean Circulation, Sea Level, and Neotectonics) and funded by the German Science Foundation (DFG) as part of the EUROMARGINS/EUROCORES program. Plutur samples were collected by the Hydrographic Institute of Portugal in cooperation with the Department of Geology and Oceanography (DGO) of the University Bordeaux during the European OMEX (Ocean Margin Exchange) program. We thank F. Abrantes, I. M. Gil, E. Salgueiro for thorough, valuable discussions, G.J. Weltje for providing the end-member modelling algorithm, Monika Segl, Birgit Meyer-Schack, Hella Buschhoff and the crew of RV *POSEIDON* during leg 304 for technical support and Phillip Franke for assistance with the grain-size measurements.

References

- Abrantes, F., Moita, M.T., 1999. Water column and recent sediment data on diatoms and coccolithophorids, off Portugal, confirm sediment record of upwelling events. *Oceanol. Acta* 22 (3), 319–336.
- Abrantes, F., Lebreiro, S., Rodrigues, T., Gil, I., Bartels-Jónsdóttir, H., Oliveira, P., Kissel, C., Grimalt, J.O., 2005. Shallow-marine sediment cores record climate variability and earthquake activity off Lisbon (Portugal) for the last 2000 years. *Quat. Sci. Rev.* 24 (23–24), 2477–2494.
- Altabet, M.A., Francois, R., 1994. Sedimentary nitrogen isotopic ratio as a recorder for surface ocean nitrate utilization. *Glob. Biogeochem. Cycles* 8 (1), 103–116.
- Andrade, C., Freitas, M.C., Miranda, J.M., Baptista, M.A., Cachao, M., Silva, P., Munha, J., 2003. Recognizing possible tsunami sediments in the ultradissipative environment of the Tagus Estuary (Portugal). *Coastal Sediments, Clearwater Beach, Florida, USA*.
- Baptista, M.A., Miranda, J.M., Chierici, F., Zitellini, N., 2003. New study of the 1755 earthquake source based on multi-channel seismic survey data and tsunami modeling. *Nat. Hazards Earth Syst. Sci.* 3, 333–340.
- Bartels-Jónsdóttir, H.B., Knudsen, K.L., Abrantes, F., Lebreiro, S., Eiriksson, J., 2006. Climate variability during the last 2000 years in the Tagus Prodela, western Iberian Margin: benthic foraminifera and stable isotopes. *Mar. Micropaleontol.* 59 (2), 83–103.
- Blott, S.J., Pye, K., 2001. Gradstat: a grain-size distribution and statistics package for the analysis of unconsolidated sediments. *Earth Surf. Processes Landf.* 26, 1237–1248.
- Bonway, H.C., Mix, A.C., 2004. Oxygen isotopes, upper ocean salinity and precipitation sources in the eastern tropical Pacific. *Earth Planet. Sci. Lett.* 224, 493–507.
- Castanheiro, J.M., 1982. Distribution, transport and sedimentation of suspended matter in the Tejo Estuary. *Estuarine Processes: an Application to the Tagus estuary*, Proceedings of a UNESCO/IOC/CNA workshop, Palácio Foz, Lisbon, Portugal.
- Cook, E.R., D'Arrigo, R.D., Mann, M.E., 2002. A well-verified, multiproxy reconstruction of the winter North Atlantic Oscillation index since A.D. 1400. *J. Clim.* 15, 1754–1764.
- Desprat, S., Sánchez-Goni, M.F., Loutre, M.F., 2003. Revealing climatic variability of the last three millennia in northwestern Iberia using pollen influx data. *Earth Planet. Sci. Lett.* 213, 63–78.
- Eiriksson, J., Bartels-Jónsdóttir, H.B., Cage, A.G., Gudmundsdóttir, E.R., Klitgaard-Kristensen, D., Marret, F., Rodrigues, T., Abrantes, F., Austin, W.E.N., Jiang, H., Knudsen, K.-L., Sejrup, H.-P., 2006. Variability of the North Atlantic Current during the last 2000 years based on shelf bottom water and sea surface temperatures along an open ocean/shallow marine transect in western Europe. *Holocene* 16 (7), 1017–1029.
- Fiúza, A.F.G., 1983. Upwelling patterns off Portugal. In: Suess, E., Thiede, J. (Eds.), *Coastal Upwelling: Its Sediment Record*. Plenum, New York, pp. 85–98.
- Folk, R.L., Ward, W.C., 1957. Brazos River bar: a study in the significance of grain-size parameters. *J. Sediment. Petrol.* 27, 3–26.
- Freitas, M.C., Andrade, C., Moreno, J.C., Munhá, J.M., Cachao, M., 1999. The sedimentary record of recent (last 500 years) environmental changes in the Seixal Bay marsh, Tagus Estuary, Portugal. *Geol. Mijnb.* 77, 283–293.
- Freudenthal, T., Neuer, S., Meggers, H., Davenport, R., Wefer, G., 2001. Influence of lateral particle advection and organic matter degradation on sediment accumulation and stable nitrogen isotope ratios along a productivity gradient in the Canary Islands region. *Mar. Geol.* 177 (1–2), 93–109.

- Gil, I.M., Abrantes, F., Hebbeln, D., 2006. The North Atlantic Oscillation forcing through the last 2000 years: spatial variability as revealed by high-resolution marine diatom records from N and SW Europe. *Mar. Micropaleontol.* 60 (2), 113–129.
- Guerzoni, S., Molinaroli, E., Chester, R., 1997. Saharan dust inputs to the western Mediterranean Sea: depositional patterns, geochemistry and sedimentological implications. *Deep-sea Res. II* 44 (3–4), 631–654.
- Hebbeln, D., Knudsen, K.-L., Gyllencreutz, R., Kristensen, P., Klitgaard-Kristensen, D., Backman, J., Scheurle, C., Jiang, H., Gil, I., Smelror, M., Jones, P.D., Sejrup, H.-P., 2006. Late Holocene coastal hydrographic and climate changes in the eastern North Sea. *Holocene* 16 (7), 987–1001.
- Holz, C., Stuut, J.B.W., Henrich, R., 2004. Terrigenous sedimentation processes along the continental margin off NW Africa: implications from grain-size analysis of seabed sediments. *Sedimentology* 51, 1145–1154.
- Hurrell, J.W., 1995. Decadal trends in the North Atlantic Oscillation: regional temperatures and precipitation. *Science* 269, 676–679.
- Jouanneau, J.M., Garcia, C., Oliveira, A., Rodrigues, A., Dias, J.A., Weber, O., 1998. Dispersal and deposition of suspended sediment on the shelf off the Tagus and Sado estuaries, S.W. Portugal. *Prog. Oceanogr.* 42, 233–257.
- Koopmann, B., 1981. Sedimentation von Saharastaub im subtropischen Nordatlantik während der letzten 25.000 Jahre. *Meteor.-Forsch.ergeb., C Geol. Geophys.* (35), 23–59.
- Lavik, G., 2001. Nitrogen Isotopes of sinking matter and sediments in the South Atlantic. Ph.D. Thesis, Fachbereich Geowissenschaften, Bremen, 140 pages.
- Lebreiro, S.M., Francés, G., Abrantes, F.F.G., Diz, P., Bartels-Jónsdóttir, H.B., Stroynowski, Z.N., Gil, I.M., Pena, L.D., Rodrigues, T., Jones, P.D., Nombela, N.A., Alejo, L., Briffa, K.R., Harris, I., Grimalt, J.O., 2006. Climate change and coastal hydrographic response along the Atlantic Iberian margin (Tagus Prodelta and Muros Ria) during the last two millennia. *Holocene* 16 (7), 1003–1015.
- Liu, K.-K., Kaplan, I.R., 1989. The eastern tropical Pacific as a source of ^{15}N -enriched nitrate in seawater off southern California. *Limnol. Oceanogr.* 34 (5), 820–830.
- Mahowald, N., Kohlfled, K., Hansson, M., Balkanski, Y., Harrison, S.P., Prentice, I.C., Schulz, M., Rodhe, H., 1999. Dust sources and deposition during the last glacial maximum and current climate: a comparison of model results with paleodata from ice cores and marine sediments. *J. Geophys. Res.* 104 (D13), 15895–15916.
- Mariotti, A., 1983. Atmospheric nitrogen is a reliable standard for natural N-15 abundance measurements. *Nature* 303 (5919), 685–687.
- Martins, V., Jouanneau, J.M., Weber, O., Rocha, F., 2006. Tracing the late Holocene evolution of the NW Iberian upwelling system. *Mar. Micropaleontol.* 59 (1), 35–55.
- McCrea, J.M., 1950. On the isotopic chemistry of carbonates on a paleotemperature scale. *J. Chem. Phys.* 18, 849–857.
- Middelburg, J.J., Nieuwenhuize, J., 1998. Carbon and nitrogen stable isotopes in suspended matter and sediments from the Schelde estuary. *Mar. Chem.* 60 (3–4), 217–225.
- Moreno, A., Cacho, I., Canals, M., Prins, M.A., Sánchez-Goñi, M.F., Grimalt, J.O., Weltje, G. J., 2002. Saharan dust transport and high-latitude glacial climatic variability: the Alboran Sea record. *Quat. Res.* 58 (3), 318–328.
- Müller, P., Schneider, R.R., Ruhland, G., 1994. Late Quaternary pCO_2 variations the Angola Current: evidence from organic carbon $\delta^{13}\text{C}$ and alkenone temperatures. In: Zahn, R., et al. (Ed.), *Carbon Cycling in the Glacial Ocean: Constraints of the Ocean's Role in Global Change*. NATO ASI Series, vol. 1(17). Springer, pp. 343–366.
- Nadeau, M.-J., Schleicher, M., Grootes, P.M., Erlenkeuser, H., Gottang, A., Mous, D.J.W., Sarthain, J.M., Willkomm, H., 1997. The Leibniz-Labor AMS facility at the Christian-Albrechts University, Kiel, Germany. *Nucl. Instrum. Methods Phys. Res. Sect. B* 132 (1–4), 22–30.
- Niebler, H.-S., Hubberten, H.-W., Gersonde, R., 1999. Oxygen isotope values of planktonic foraminifera: a tool for the reconstruction of surface water stratification. In: Fischer, G., Wefer, G. (Eds.), *Use of Proxies in Paleoceanography: Examples from the South Atlantic*. Springer Verlag, Berlin, Heidelberg, pp. 165–189.
- Oschlies, A., 2001. NAO-induced long-term changes in nutrient supply to the surface waters of the North Atlantic. *Geophys. Res. Lett.* 28 (9), 1751–1754.
- Owens, N.J.P., 1985. Variations in the natural abundance of ^{15}N in estuarine suspended particulate matter: a specific indicator of biological processing. *Estuar. Coast. Shelf Sci.* 20, 505–510.
- Prins, M.A., 1999. Pelagic, hemipelagic and turbidite deposition in the Arabian Sea during the late Quaternary: unravelling the signals of eolian and fluvial sediment supply as functions of tectonics, sea-level and climate change by means of end-member modelling of siliciclastic grain-size distributions – PhD thesis, Utrecht, Utrecht University. *Geologica Ultraiectina* 168, 1–192.
- Prins, M.A., Weltje, G.J., 1999. End-member modeling of siliciclastic grain-size distributions: the late Quaternary record of eolian and fluvial sediment supply to the Arabian Sea and its paleoclimatic significance. In: Harbaugh, J., et al. (Ed.), *Numerical Experiments in Stratigraphy: Recent Advances in Stratigraphic and Sedimentologic Computer Simulations*, SEPM (Society for Sedimentary Geology). Special Publication, vol. 62, pp. 91–111.
- Schubert, C.J., Nielsen, B., 2000. Effects of decarbonation treatments on $\delta^{13}\text{C}$ values in marine sediments. *Mar. Chem.* 72, 55–59.
- Scourse, J., Sejrup, H.P., Jones, P.D., HOLSMEER project participants, 2006. Editorial: Late Holocene oceanographic and climate change from the western European margin: the results of the HOLSMEER project. *Holocene* 16 (7), 931–935.
- Stuiver, M., Reimer, P.J., 1993. Extended 14C database and revised CALIB radiocarbon calibration program. *Radiocarbon* 35, 215–230.
- Stuut, J.B.W., Prins, M.A., Schneider, R.R., Weltje, G.J., Jansen, J.H.F., Postma, G., 2002. A 300-kyr record of aridity and wind strength in southwestern Africa: inferences from grain-size distributions of sediments on Walvis Ridge, SE Atlantic. *Mar. Geol.* 180 (1–4), 221–233.
- Thornton, S.F., McManus, J., 1994. Application of organic carbon and nitrogen stable isotope and C/N ratios as source indicators of organic matter provenance in estuary systems: evidence from the Tay Estuary, Scotland. *Estuar. Coast. Shelf Sci.* 38, 219–233.
- Trigo, R., Pozo-Vázquez, D., Osborn, T., Castro-Diez, Y., Ganiz-Fortis, S., Esteban-Parra, M.J., 2004. North Atlantic Oscillation influence on precipitation, river flow and water resources in the Iberian Peninsula. *Int. J. Climatol.* 24, 925–944.
- Vicente-Serrano, M., Heredia-Laclaustra, A., 2004. NAO influence on NDVI trends in the Iberian Peninsula (1982–2000). *Int. J. Remote Sens.* 25 (14), 2871–2879.
- Weltje, G.J., 1997. End-member modeling of compositional data: numerical-statistical algorithms for solving the explicit mixing problem. *J. Math. Geol.* 29, 503–549.
- Weltje, G.J., Prins, M.A., 2003. Muddled or mixed? Inferring palaeoclimate from size distributions of deep-sea clastics. *Sediment. Geol.* 162 (1–2), 39–62.
- Wolff, T., Grieger, B., Hale, W., Dürkopp, A., Mulitza, S., Pätzold, J., Wefer, G., 1999. On the reconstruction of paleosalinities. In: Fischer, G., Wefer, G. (Eds.), *Use of Proxies in Paleoceanography: Examples from the South Atlantic*. Springer Verlag, Berlin, Heidelberg, pp. 207–228.